Fursultiamine Alleviates Choroidal Neovascularization by Suppressing Inflammation and Metabolic Reprogramming

Ji Yeon Do,[1] Juhee Kim,[1] Mi-Jin Kim,[1] Jung Yi Lee,[1,2] So-Young Park,[3] Ryoji Yanai,[4] In-Kyu Lee,[1,5] Sungmi Park,[1] and Dong Ho Park[1,6]

[1]Leading-Edge Research Center for Drug Discovery and Development for Diabetes and Metabolic Disease, Kyungpook National University Hospital, Kyungpook National University, Daegu, Republic of Korea
[2]R&D Center, JD Bioscience, Inc., Gwangju, Republic of Korea
[3]College of Pharmacy and Research Institute of Pharmaceutical Sciences, Kyungpook National University, Daegu, Republic of Korea
[4]Department of Ophthalmology, Yamaguchi University Graduate School of Medicine, Ube, Yamaguchi, Japan
[5]Department of Internal Medicine, School of Medicine, Kyungpook National University Hospital, Kyungpook National University, Daegu, Republic of Korea
[6]Department of Ophthalmology, School of Medicine, Kyungpook National University Hospital, Kyungpook National University, Daegu, Republic of Korea

Correspondence: Dong Ho Park, Department of Ophthalmology, School of Medicine, Kyungpook National University Hospital, Kyungpook National University, 130 Dongdeok-ro, Jung-gu, Daegu 41944, Republic of Korea; dongho_park@knu.ac.kr.
Sungmi Park, Leading-Edge Research Center for Drug Discovery and Development for Diabetes and Metabolic Disease, Kyungpook National University Hospital, Kyungpook National University, 807 Hoguk-ro, Buk-gu, Daegu 41404, Republic of Korea; smpark93@gmail.com.

Received: June 5, 2020
Accepted: October 4, 2020
Published: October 27, 2020

Citation: Do JY, Kim J, Kim M-J, et al. Fursultiamine alleviates choroidal neovascularization by suppressing inflammation and metabolic reprogramming. *Invest Ophthalmol Vis Sci.* 2020;61(12):24. https://doi.org/10.1167/iovs.61.12.24

Purpose. To assess the therapeutic effects of fursultiamine on choroidal neovascularization (CNV) through its modulation of inflammation and metabolic reprogramming in the retinal pigment epithelium (RPE).

Methods. The anti-angiogenic effects of fursultiamine were assessed by measuring vascular leakage and CNV lesion size in the laser-induced CNV mouse model. Inflammatory responses were evaluated by quantitative polymerase chain reaction, western blot, and ELISA in both CNV eye tissues and in vitro cell cultures using ARPE-19 cells or primary human RPE (hRPE) cells under lipopolysaccharide (LPS) treatment or hypoxia. Mitochondrial respiration was assessed by measuring oxygen consumption in ARPE-19 cells treated with LPS with or without fursultiamine, and lactate production was measured in ARPE-19 cells subjected to hypoxia with or without fursultiamine.

Results. In laser-induced CNV, fursultiamine significantly decreased vascular leakage and lesion size, as well as the numbers of both choroidal and retinal inflammatory cytokines, including IL-1β, IL-6, IL-8, and TNF-α. In LPS-treated ARPE-19 cells, fursultiamine decreased proinflammatory cytokine secretion and nuclear factor kappa B phosphorylation. Furthermore, fursultiamine suppressed LPS-induced upregulation of IL-6, IL-8, and monocyte chemoattractant protein-1 in a dose-dependent and time-dependent manner in primary hRPE cells. Interestingly, fursultiamine significantly enhanced mitochondrial respiration in the LPS-treated ARPE-19 cells. Additionally, fursultiamine attenuated hypoxia-induced aberrations, including lactate production and inhibitory phosphorylation of pyruvate dehydrogenase. Furthermore, fursultiamine attenuated hypoxia-induced VEGF secretion and mitochondrial fission in primary hRPE cells that were replicated in ARPE-19 cells.

Conclusions. Our findings show that fursultiamine is a viable putative therapeutic for neovascular age-related macular degeneration by modulating the inflammatory response and metabolic reprogramming by enhancing mitochondrial respiration in the RPE.

Keywords: choroidal neovascularization, inflammation, metabolic reprogramming, mitochondria, fursultiamine

Age-related macular degeneration (AMD) is the most common cause of blindness in the elderly.[1] The neovascular form of AMD is characterized by choroidal neovascularization (CNV), in which premature vessels extend through the retinal pigment epithelium (RPE) into the retina.[2] CNV causes edema and bleeding, followed by destruction of photoreceptors and loss of vision. Because apical photoreceptor outer segments are continuously shedding, the RPE must phagocytose and degrade shed outer segments throughout life.[3] To do so, the RPE requires a significant energy supply, which is supported by a robust mitochondrial network.[4] However, due to degeneration and apoptosis with aging, RPE density declines, as does the cellular capacity to degrade phagocytosed outer segments.[5,6] This disrupted homeostasis causes progressive accumulation of intracellular lipofuscin, resulting in mitochondrial dysfunction,

which can generate a proinflammatory environment around the RPE, promoting the development and progression of AMD.[7]

Release of inflammatory cytokines from the RPE contributes to CNV,[5] and these cytokines, including IL-6, IL-8, monocyte chemoattractant protein-1 (MCP-1), and TNF-α, are regulated by nuclear factor kappa B (NF-κB), a master regulator of inflammation.[8–11] Under hypoxic or inflammatory conditions, stabilized hypoxia-inducible factor 1-alpha (HIF-1α) plays an important role in metabolic reprogramming from oxidative phosphorylation (OXPHOS) toward aerobic glycolysis, a process that results in the release of proinflammatory cytokines, including IL-1β.[12,13] Thus, we hypothesized that intracellular stress in the RPE under the hypoxic and proinflammatory microenvironment of AMD could reprogram RPE metabolism from OXPHOS to aerobic glycolysis. Considering the link between proinflammatory cytokines and CNV development, RPE metabolic reprogramming could be a novel therapeutic target for neovascular AMD.

Thiamine, or vitamin B1, is a cofactor of mitochondrial pyruvate dehydrogenase (PDH), which is an important enzyme for OXPHOS.[14] Several synthetic lipophilic derivatives have been developed to increase the bioavailability of thiamine, such as benfotiamine, and the most recent derivative, fursultiamine.[15] Prior studies have demonstrated that benfotiamine significantly reduces secretion of proinflammatory cytokines in lipopolysaccharide (LPS)-activated macrophages[16] and microglia,[17] which is mediated by suppression of NF-κB signaling. However, the effects of fursultiamine on the inflammatory and metabolic responses of the RPE have not been investigated, especially in the context of CNV. Thus, the present study evaluated whether fursultiamine alleviated CNV by modulating RPE inflammatory and metabolic responses in the mouse laser-induced CNV model.

Methods

Animal Experiments

All mouse experiments were performed in accordance with the guidelines of the ARVO Statement for the Use of Animals in Ophthalmic and Vision Research and were approved by the Animal Care Committee of Kyungpook National University (no. 2019-0104-1).

Cell Culture

This study used the human RPE cell line ARPE-19 (CLR-2302; American Type Culture Collection, Manassas, VA, USA) between 25 and 27 passages and primary human RPE (hRPE) cells (Lonza, Walkersville, MD, USA) between 5 and 6 passages. ARPE-19 cells were cultured in Dulbecco's Modified Eagle Medium/Nutrient Mixture F-12 (DMEM/F12) supplemented with 10% fetal bovine serum (FBS) and 100 U/mL penicillin/100 µg/mL streptomycin (P/S) and passaged at ratios of 1:2 to 1:4 using trypsin–EDTA (Thermo Fisher Scientific, Waltham, MA, USA). Primary hRPE cells were cultured in basal media containing supplements (RtEGM BulletKit; Lonza). For subculture, 2% FBS was added to the media, and the media were replaced with serum-free media after 24 hours. Cells were treated with 10 µg/mL LPS (*Escherichia coli* O111:B4; Sigma-Aldrich, St. Louis, MO, USA) with or without fursultiamine–HCl (Toronto Research Chemicals, North York, ON, Canada) at the specified concentrations. Confluent ARPE-19 cells were maintained in a medium consisting of DMEM/F12, 1% FBS, 1.5 mM pyruvate, and 1% P/S for mitochondrial activation, as described previously.[18] The medium was changed every 2 days through days 4 to 6.

Laser-Induced CNV Model and Drug Administration

Male C57BL/6J mice at 8 weeks of age were used for all experiments. A 532-nm OcuLight GLx laser system (Iridex Corporation, Mountain View, CA, USA) attached to a slit lamp was used to generate CNV lesions. According to the method described in previous studies,[19,20] four lesions were generated with the following laser parameters: 100-mW power, 100-µm spot size, and 0.1-second pulse duration. The appearance of a bubble at the site of photocoagulation signified successful disruption of the Bruch's membrane. Retina and RPE/choroid tissues were collected at the specified time points for RNA isolation or choroidal flat-mount. Mice were treated with fursultiamine (50 mg/kg) or saline vehicle by oral gavage once daily beginning 7 days prior (day –7) to CNV induction (day 0) through day +7 after CNV induction.

Choroidal Flat-Mounts

At 7 days after CNV induction, eyes were enucleated and fixed in 4% paraformaldehyde for 30 minutes. Retinas were then removed from the underlying choroid and sclera to generate the choroidal flat-mount. Alexa Fluor 488 conjugated to isolectin B4 (1:100; Thermo Fisher Scientific) was used to stain eyecups overnight at 4°C. PermaFluor Aqueous Mounting Medium (Thermo Fisher Scientific) was then used to flat-mount the eyecup with the choroid facing upward and the sclera facing downward. Flat-mount images were captured using an LSM 800 with Airyscan detector (Carl Zeiss Microscopy GmbH, Jena, Germany), and ImageJ software (National Institutes of Health, Bethesda, MD, USA) was used to measure the CNV lesion size followed by the analysis described in previous studies.[19,20]

Fluorescein Angiography

A Micron IV retinal imaging microscope (Phoenix Technology Group, Pleasanton, CA, USA) was used to capture fluorescein images. After anesthesia and pupil dilation, images were obtained 3 to 5 minutes (early phase) and 7 to 10 minutes (late phase) after intraperitoneal injection of 0.1 mL 2% fluorescein sodium (Akorn, Inc., Lake Forest, IL, USA) using StreamPix software (NorPix, Montreal, QC, Canada). A previously described scheme was used to grade the lesions: faint or mottled fluorescence without leakage was scored as 0 (no leakage); hyperfluorescence without increase in size or intensity was scored as 1 (mild leakage); hyperfluorescence with constant size but increasing intensity was scored as 2A (moderate leakage); and hyperfluorescence with increasing size and intensity was scored as 2B (clinically significant leakage).[19,20]

Quantitative Real-Time Polymerase Chain Reaction

Total RNA was extracted from mouse tissue using QIAzol lysis reagent (Qiagen, Hilden, Germany) following the

Investigative Ophthalmology & Visual Science

manufacturer's instructions. Total RNA was used for cDNA synthesis using a cDNA synthesis kit (Thermo Fisher Scientific). Quantitative real-time polymerase chain reaction (qPCR) analysis was performed with SYBR Green master mix (Thermo Fisher Scientific) using the ViiA 7 Real-Time PCR System (Applied Biosystems, Carlsbad, CA, USA).

Specific primers used for real-time PCR were as follows: mouse IL-1β, 5′-AGTTGACGGACCCCAAAAGAT-3′ (forward) and 5′-GTTGATGTGCTGCTGCGAGA-3′ (reverse); mouse IL-6, 5′-AAGTCGGAGGCTTAATTACACATGT-3′ (forward) and 5′-CCATTGCACAACTCTTTTCTCATT-3′ (reverse); mouse IL-8, 5′-GGATGGGAACAACGATAGGAAAT-3′ (forward) and 5′-ATCTCTGTCTCTCTGCACCTCACTT-3′ (reverse); mouse TNF-α, 5′-GACGTGGAACTGGCAGAAGA-3′ (forward) and 5′-CCGCCTGGAGTTCTGGAA-3′ (reverse); and mouse 36B4, 5′-ACCTCCTTCTTCCAGGCTTT-3′ (forward) and 5′-CTCCAGTCTTTATCAGCTGC-3′ (reverse). Target gene levels were normalized using 36B4 as an internal control.

Western Blot Analysis

ARPE-19 cells were lysed with lysis buffer (20 mM Tris, pH 7.4; 10 mM Na_4P_2OH; 100 mM NaF; 2 mM Na_3VO_4; 5 mM EDTA, pH 8.0; 0.1 mM phenylmethylsulfonyl fluoride; and 1% NP-40) containing protease inhibitors (aprotinin 7 µg/mL and leupeptin 7 µg/mL) and a phosphatase inhibitor cocktail (Sigma-Aldrich). Protein concentrations were measured using the BCA Protein Assay Kit (Thermo Fisher Scientific). Cell lysates were separated by 10% sodium dodecyl sulfate–polyacrylamide gel electrophoresis, and the resolved proteins were transferred to polyvinylidene difluoride membranes (MilliporeSigma, Burlington, MA, USA). Membranes were immunoblotted with the following primary antibodies: anti-phospho-NF-κB (Cell Signaling Technology, Danvers, MA, USA); anti-NF-κB (Cell Signaling Technology); anti-phospho-IκB (Cell Signaling Technology); anti-IκB (Cell Signaling Technology); anti-heat shock protein 90 (HSP90) (Cell Signaling Technology); anti-hypoxia-inducible factor 1-alpha (HIF-1α) (Novus Biologicas, Littleton, CO, USA); anti-phospho-pyruvate dehydrogenase (PDH; S293, S232, and S300) (MilliporeSigma), and anti-β-actin (Sigma-Aldrich). HSP90 and β-actin were used as loading controls.

Enzyme-Linked Immunosorbent Assay for Cytokines

Secreted levels of IL-6, IL-8, MCP-1, and VEGF in cell culture media from ARPE-19 cells and primary hRPE cells were measured using ELISA kits (R&D Systems, Minneapolis, MN, USA), according to the manufacturer's instructions.

Measurement of Oxygen Consumption Rate

The oxygen consumption rate (OCR) was measured using an XFe96 Extracellular Flux Analyzer (Seahorse Bioscience, Inc., Billerica, MA, USA). ARPE-19 cells were seeded in XFe96 cell culture plates (96-well) at a density of 2×10^4 cells/well and incubated overnight. On day 6, the ARPE-19 cells were treated with LPS (10 µg/mL) for 48 hours with or without fursultiamine for the final 24 hours. The assay medium consisted of XF DMEM Medium pH 7.4 (Agilent Technologies, Santa Clara, CA, USA) supplemented with 5.5 mM Seahorse XF 1.0 M glucose solution, 9 mM Seahorse XF 100 mM pyruvate solution, and 1 mM Seahorse XF 200 mM glutamine solution. Sigma-Aldrich inhibitors and uncouplers were used at the following concentrations: oligomycin A (1 µM), carbonyl cyanide 4-(trifluoro-methoxy) phenylhydrazone (FCCP, 0.5 µM), rotenone (1 µM), and antimycin A (1 µM). To normalize by cell number, 4′,6-diamidino-2-phenylindole (DAPI)-stained cells were counted automatically by ImageXpress Micro Confocal Microscopy (Molecular Devices, San Jose, CA, USA).

L-Lactate Assay

Cells were exposed to hypoxic (1% O_2) conditions with or without fursultiamine treatment. After 12 hours, the media were collected for measurement of L-lactate. Extracellular lactate was measured using an EnzyChrom L-Lactate Assay Kit (BioAssay Systems, Hayward, CA, USA) according to the manufacturer's instructions.

Immunofluorescence for Mitochondrial Morphology

Primary hRPE cells and ARPE-19 cells were pretreated with fursultiamine followed by incubation in an Invivo$_2$ 400 workstation (The Baker Company, Sanford, ME, USA). After 12 hours, cells were fixed with 4% paraformaldehyde and subsequently permeabilized in PBS with 0.1% Triton X-100 (Sigma-Aldrich) and 0.1 M glycine. After they were washed with PBS, cells were incubated with primary antibody against translocase of outer mitochondrial membrane 20 (Tom20) (Santa Cruz Biotechnology, Santa Cruz, CA, USA) overnight at 4°C. Alexa Fluor 594 goat anti-rabbit secondary antibody (Thermo Fisher Scientific) was used as secondary antibody and was incubated for 2 hours at room temperature. Cells were mounted in VECTASHIELD mounting medium with DAPI (Vector Laboratories, Inc., Burlingame, CA, USA). Images of primary hRPE cells were acquired using an ImageXpress Micro Confocal High-Content Imaging System (Molecular Devices) with a 100× Plan Fluor objective in confocal mode (60 mm pinhole spinning). A 3 mm z-stack with 0.6 mm between image planes was obtained using DAPI and Texas Red. A two-dimensional projection was created to represent maximum intensity and processed using the "Flatten Background" function to provide clear mitochondrial structures using MetaXpress (Molecular Devices). Images for ARPE-19 cells were acquired using a Zeiss LSM 800 confocal camera.

Pharmacokinetic Study

A pharmacokinetic study was conducted to assess the bioavailability of fursultiamine. A retro-orbital blood sample was taken from anesthetized mice receiving once-daily injections of fursultiamine (50 mg/kg) on days 1, 7, and 14 after beginning treatment, 2 hours after oral gavage. Blood levels of thiamine and thiamine pyrophosphate were analyzed by liquid chromatography–tandem mass spectrometry (LC-MS/MS 8060 system; Shimadzu, Kyoto, Japan).

Statistical Analysis

Data were presented using Prism 6.0 (GraphPad Software, San Diego, CA, USA), and statistical analyses were performed using SPSS Statistics 21.0 (IBM, Armonk, NY, USA). Results are expressed as mean ± SEM. A two-sample t-test was used

Investigative Ophthalmology & Visual Science

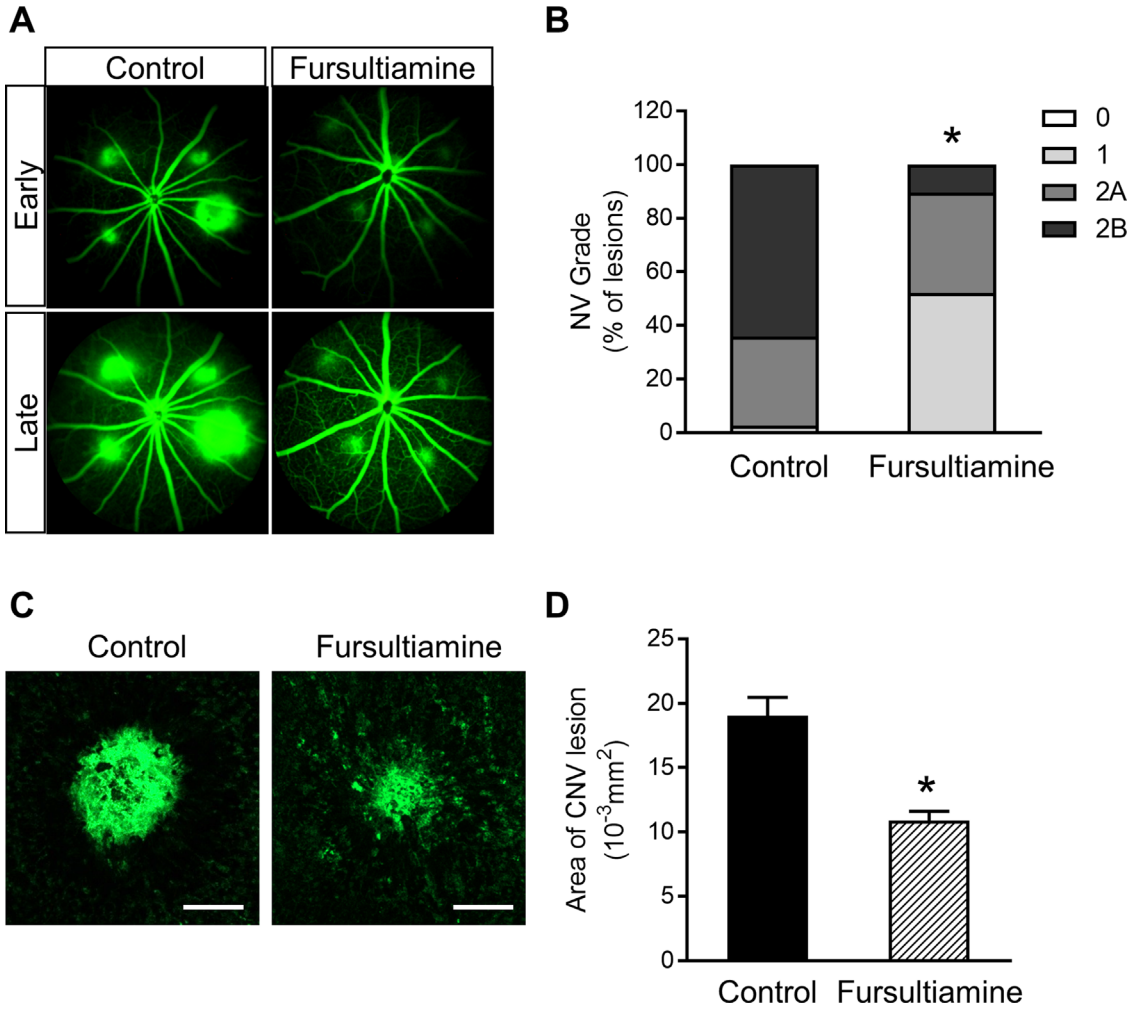

Figure 1. Therapeutic effect of fursultiamine in the laser-induced CNV model. (**A**, **B**) CNV lesion grading (0, 1, 2A, and 2B) was conducted in fluorescein angiography images from control and fursultiamine-treated CNV mice 7 days after CNV induction. (**C**, **D**) CNV lesion size was calculated in both groups. $^{*}P < 0.05$ versus control ($n = 30$ lesions/group). *Scale bar*: 100 µm.

to compare two groups. Multiple-group comparison was performed by one-way ANOVA, followed by Tukey's multiple comparison tests. Statistical significance was defined as $P < 0.05$.

Results

Fursultiamine Decreased CNV Severity and Expression of Inflammatory Cytokines

To assess the therapeutic potential of fursultiamine in neovascular AMD, we evaluated the effects of oral fursultiamine administration on laser-induced CNV mice. On day 7 after CNV induction, the proportion of grade 2B lesions, defined as exhibiting clinically significant vascular leakage, was significantly decreased in the fursultiamine-treated CNV group relative to the control CNV group (Figs. 1A, 1B). Further, CNV lesion size was decreased in CNV mice treated with fursultiamine relative to control CNV mice, as assessed by choroidal flat-mount (Figs. 1C, 1D). A pharmacokinetic study of circulating thiamine and its active metabolite thiamine pyrophosphate demonstrated that plasma levels of these molecules reached high concentrations 1 day after initiating oral administration of fursultiamine (50 mg/kg) (Supplementary Fig. S1). These findings suggested that fursultiamine alleviated abnormal outgrowth of the choroidal vasculature and decreased vascular leakage in the CNV model.

Inflammatory cytokines, including IL-1β, MCP-1, and TNF-α, are highly expressed in both human CNV tissues and in the laser-induced CNV mouse model.[21,22] Thus, we measured mRNA levels of TNF-α, IL-6, IL-1β, and IL-8 in choroids and retinas from CNV mice with and without fursultiamine 3 hours, 1 day, and 3 days post-CNV induction. Fursultiamine decreased choroidal mRNA levels of IL-6 and IL-1β on day 1 and IL-8 on day 3 post-CNV induction (Fig. 2A). Furthermore, fursultiamine decreased the retinal levels of TNF-α at 3 hours, IL-1β on day 1, and IL-6 on day 3 post-CNV induction (Fig. 2B). Interestingly, this significant difference was not detected at other time points (Supplementary Fig. S2), which could be due to the dynamic expression patterns of cytokines during the 7 days following CNV induction.[23] At day 1 post-CNV, IL-8 protein levels were decreased by fursultiamine (Supplementary Fig. S3A). At day 3, VEGF protein levels decreased with fursultiamine treatment (Supplementary Fig. S3B). Taken

Investigative Ophthalmology & Visual Science

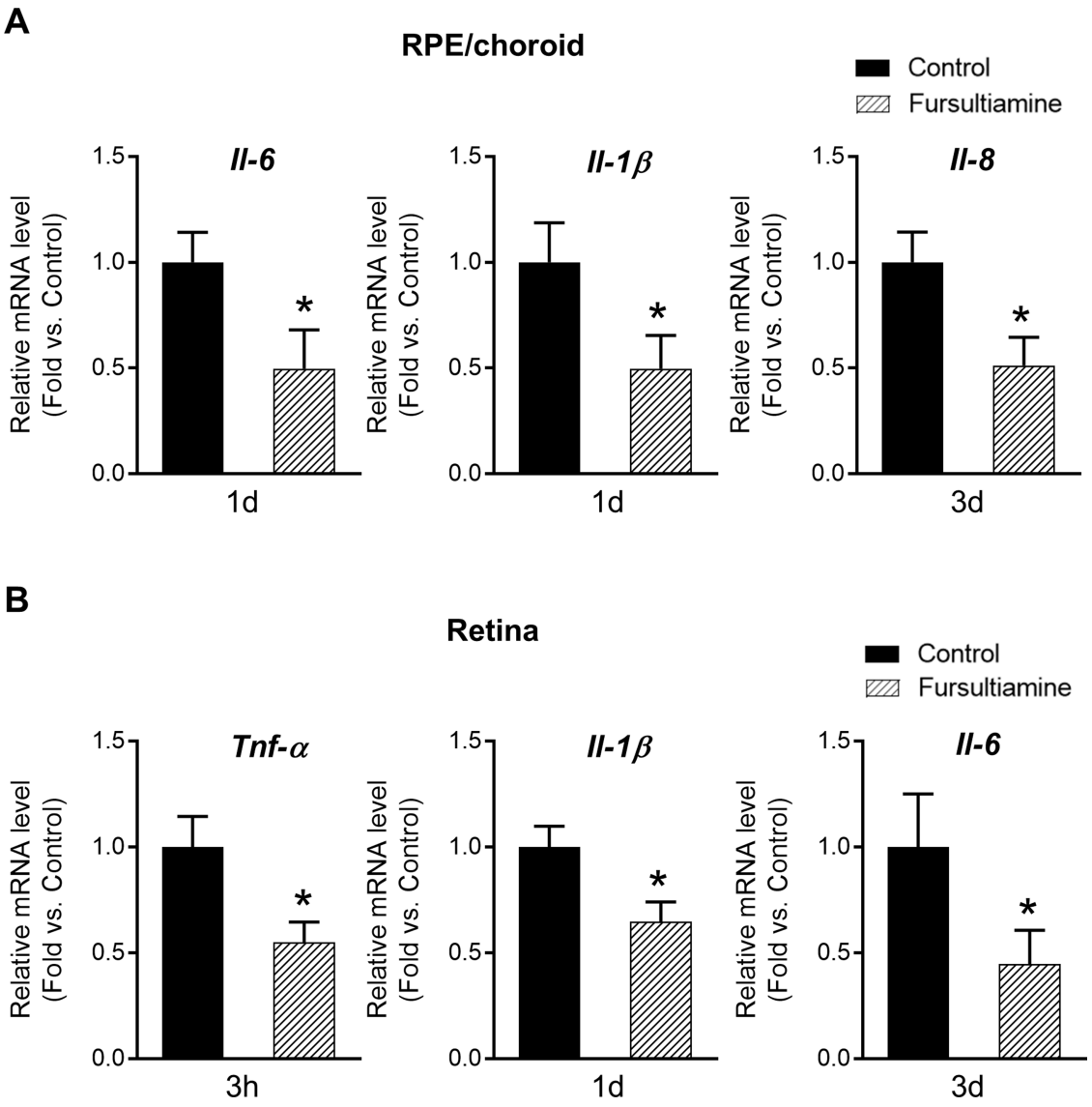

Figure 2. Downregulated choroidal and retinal inflammatory gene expression in fursultiamine-treated CNV mice. (**A**, **B**) RNA was isolated from RPE/choroids (**A**) or retinas (**B**) from control and fursultiamine groups at 3 hours, 1 day, and 3 days after CNV induction to measure mRNA expression of proinflammatory cytokines by qPCR. $^{*}P < 0.05$ versus control ($n = 3$ to 5 per group).

together, these data suggest that fursultiamine ameliorated CNV severity and suppressed inflammatory cytokines in CNV mice.

Fursultiamine Suppressed Inflammation in LPS-Induced Human RPE Cells

Because RPE-mediated production and release of cytokines under the inflammatory condition has a crucial role in CNV development, LPS stimulation of the RPE followed by cytokine release is often used to elucidate the pathological mechanism of AMD in previous studies.[24,25] Thus, we evaluated the anti-inflammatory effects of fursultiamine in LPS-treated ARPE-19 cells. Fursultiamine suppressed LPS-induced upregulation of IL-6, IL-8, and MCP-1 protein levels in a dose-dependent manner (Fig. 3A). Furthermore, in primary hRPE cells, fursultiamine suppressed LPS-induced upregulation of IL-6, IL-8, and MCP-1 protein in a dose-dependent and time-dependent manner (Supplementary Fig. S4). IL-6 and MCP-1 were consistently decreased by fursultiamine treatment over multiple time points, including at 4, 12, and 24 hours after LPS treatment, whereas IL-8 was decreased only at 4 and 12 hours. This finding was consistent with reduced choroidal and retinal mRNA levels of proinflammatory cytokines in fursultiamine-treated CNV mice.

Phosphorylated NF-κB translocates to the nucleus to activate transcription of inflammatory cytokines in ARPE-19 cells.[10] Interestingly, fursultiamine significantly suppressed LPS-induced phosphorylation of NF-κB in a dose-dependent manner and furthermore suppressed IκB phosphorylation in a dose-dependent manner (Figs. 3B, 3C; see also Supplementary Fig. S6A). These data demonstrated that fursulti-

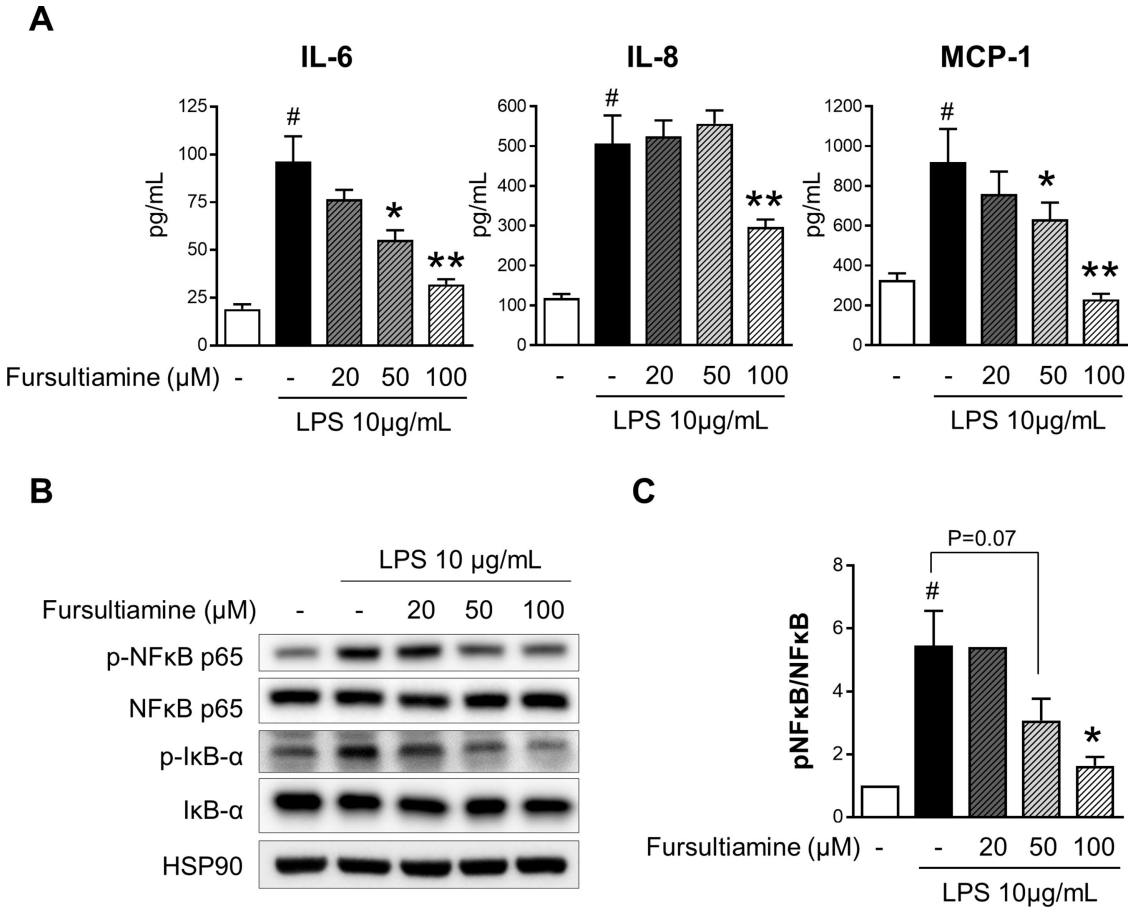

Figure 3. Decreased LPS-induced inflammatory response in fursultiamine-treated ARPE-19 cells. (**A**) Proinflammatory cytokine levels, including IL-6, IL-8, and MCP-1, were measured in media collected from ARPE-19 cells treated with LPS (10 μg/mL) with or without fursultiamine (20, 50, and 100 μM) for 12 hours. (**B**) Protein was isolated from ARPE-19 cells treated with LPS (10 μg/mL) with or without fursultiamine (20, 50, and 100 μM) for 1 hour. Lysates were subjected to immunoblotting for phosphorylated NF-κB (p-NF-κB), NF-κB, phosphorylated IκB-α (p-IκB-α), and IκB-α; $n = 6$ to 8 per experiment. (**C**) p-NF-κB and total NF-κB ratios were determined from three independent experiments by densitometry. Ratios were normalized to the p-NF-κB/t-NF-κB ratio of the control cells. $^{*}P < 0.05$ or $^{**}P < 0.001$ versus LPS only; $^{\#}P < 0.05$ versus control.

amine had an anti-inflammatory effect and suppressed NF-κB-mediated upregulation of proinflammatory cytokines.

Fursultiamine Enhanced Mitochondrial Respiration in LPS-Treated ARPE-19 Cells

The RPE is a metabolically demanding tissue, an observation that is supported by the abundance of mitochondria,[26] which demand a high degree of oxygen consumption.[27] Impaired energy metabolism and RPE dysfunction under inflammatory conditions could contribute to the development and progression of AMD. Similar to previous reports,[28] the initial mitochondrial respiration was potentiated by pyruvate supplementation compared to the basal condition (24.7 ± 2.3 vs. 13.9 ± 2.1 pmol/min/cell). To evaluate the effect of fursultiamine in metabolic reprogramming under inflammatory conditions, the OCR was measured in ARPE-19 cells treated with LPS. Interestingly, maximal respiration and spare respiratory capacity in LPS-treated cells were significantly increased with 20-μM fursultiamine, but this effect was diminished in cells treated with 50-μM fursultiamine (Fig. 4).

Fursultiamine Alleviated Hypoxia-Induced Mitochondrial Dysfunction in ARPE-19 Cells

To determine if fursultiamine modulated metabolic reprogramming under hypoxic conditions similarly to the effects observed under LPS treatment, we measured lactate and PDH levels from ARPE-19 cells subjected to hypoxia. Hypoxia-induced elevation of extracellular lactate was alleviated by fursultiamine treatment in a dose-dependent manner (Fig. 5A). Furthermore, fursultiamine significantly attenuated the hypoxia-induced increase of PDH phosphorylation (Fig. 5B; Supplementary Fig. S6B). Taken together, this suggests that fursultiamine reactivated mitochondrial PDH, which would shift mitochondrial respiration from aerobic glycolysis toward OXPHOS. Therefore, fursultiamine could improve RPE energy metabolism under hypoxia.

We next sought to determine if fursultiamine affected VEGF expression in ARPE-19, as VEGF is upregulated in the RPE cells surrounding CNV lesions in the mouse CNV model.[29] Hypoxia elevated VEGF secretion by primary hRPE cells, which was significantly attenuated by fursultiamine treatment in a dose-dependent manner (Fig. 5C). These findings were replicated in ARPE-19 cells

Investigative Ophthalmology & Visual Science

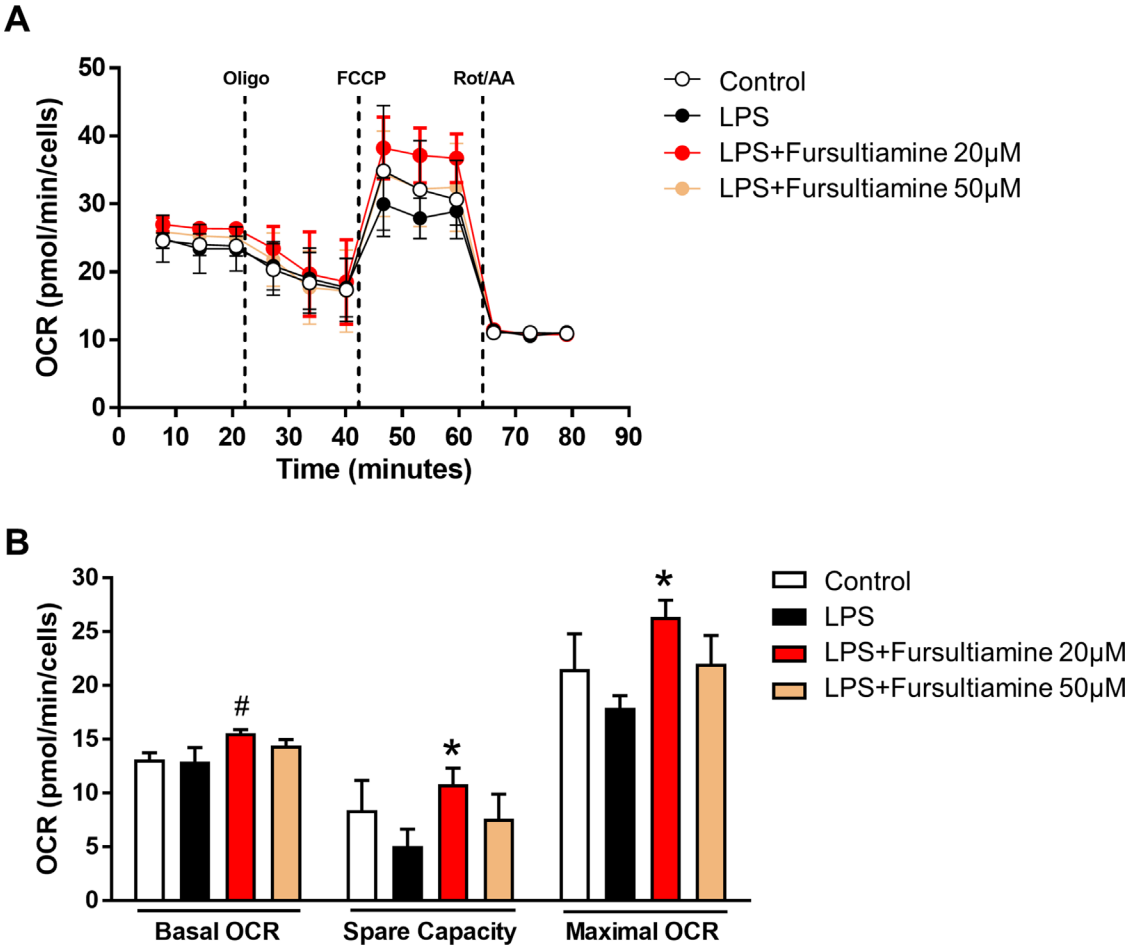

Figure 4. Improved mitochondrial function in LPS-induced ARPE-19 cells treated with fursultiamine. (**A**) The OCR was measured in ARPE-19 cells with LPS treatment for 48 hours on day 6 after pyruvate supplementation with or without fursultiamine (20 and 50 μM) for the final 24 hours. (**B**) Basal respiration, spare respiratory capacity, and maximal respiration were calculated based on the OCR response to specific inhibitors. $^{*}P < 0.05$ versus LPS only; $^{\#}P < 0.05$ versus control ($n = 6$ per group).

(Supplementary Fig. S5A). Likewise, we measured HIF-1α levels, as HIF-1α is the primary regulator of hypoxia-induced VEGF upregulation in the RPE.[30] Consistently, fursultiamine suppressed hypoxia-induced HIF-1α stabilization in a dose-dependent manner (Fig. 5D; Supplementary Fig. S6C). HIF-1α-induced VEGF secretion plays an important role in the shift toward glycolysis by orchestrating the decision to commit pyruvate to acetyl coenzyme A or to lactate.[31] Additionally, morphological mitochondrial changes were evaluated by staining with Tom20, a mitochondrial outer membrane marker. Interestingly, hypoxia induced mitochondrial fission in primary hRPE cells, which was inhibited by fursultiamine (Fig. 5E). Fursultiamine similarly affected mitochondrial morphological changes in ARPE-19 cells subjected to hypoxia (Supplementary Fig. S5B). The above data suggest that not only under inflammatory conditions but also under hypoxic conditions fursultiamine modulated metabolic reprogramming, which could be associated with its therapeutic effects in vivo.

Discussion

Thiamine, which belongs to a water-soluble vitamin B group, is an essential micronutrient for humans, although mammals cannot synthesize thiamine de novo.[32] To increase the bioavailability of thiamine, various lipophilic thiamine derivatives capable of diffusing through the plasma membrane independent of transporters, such as fursultiamine and benfotiamine, have been developed.[33,34] Although several studies reported the anti-inflammatory effects of benfotiamine, marked by decreased inflammatory cytokine expression via the NF-κB pathway,[16,17] the effect of fursultiamine, particularly in the context of CNV, had not yet been evaluated.

The present study identified therapeutic effects of fursultiamine in the laser-induced CNV mouse model of neovascular AMD, as demonstrated by decreased vascular leakage and CNV lesion size. In neovascular AMD, release of various cytokines and chemokines exacerbates pathological neovascularization.[5] IL-8 and MCP-1 are two chemokines responsible for the majority of inflammatory cytokine secretion from the RPE, which increases leukocyte chemotactic activity,[35] and they are regulated by NF-κB activation.[10,11] This study found that fursultiamine decreased expression of proinflammatory cytokines in both laser-induced CNV and human RPE cells subjected to LPS, which could be mediated by NF-κB.

A metabolic switch toward aerobic glycolysis is a common characteristic of neoplastic cells, termed the

Investigative Ophthalmology & Visual Science

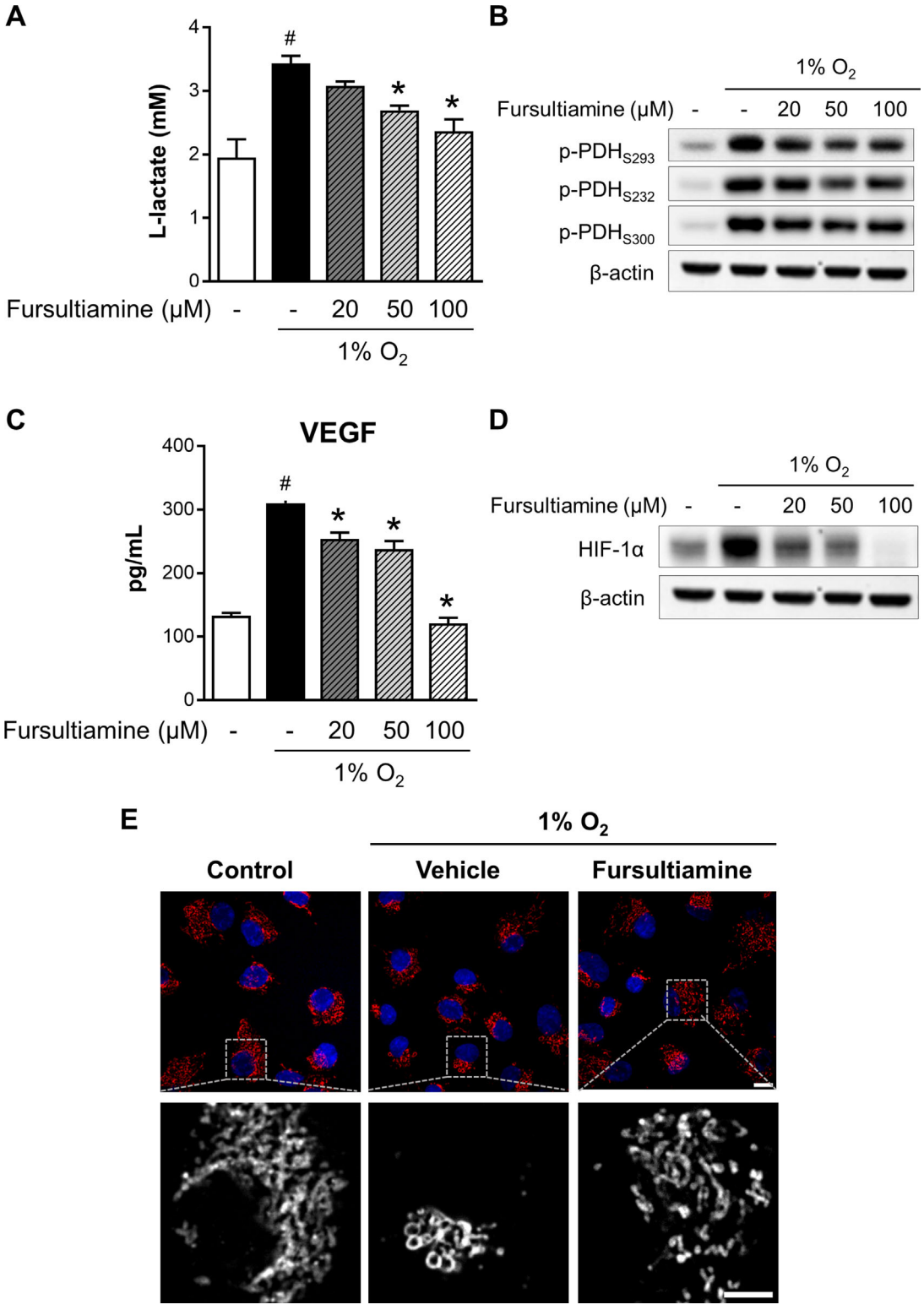

Figure 5. Beneficial effects of fursultiamine on mitochondrial dysfunction in hypoxic ARPE-19 and primary hRPE cells. (**A**) Extracellular lactate levels were measured in ARPE-19 cells under normoxic (21% O_2) and hypoxic (1% O_2) conditions with or without fursultiamine (20, 50, and 100 μM) for 12 hours. (**B**) Proteins were isolated from ARPE-19 cells subjected to hypoxia with or without fursultiamine (20, 50, and 100 μM) for 12 hours and subjected to immunoblotting for phosphorylated PDH_{S293}, PDH_{S232}, and PDH_{S300} and β-actin. (**C**) Extracellular VEGF levels were measured by ELISA in primary hRPE cells subjected to hypoxia with or without fursultiamine (50 and 100 μM) for 12 hours. (**D**) Proteins were isolated from ARPE-19 cells subjected to hypoxia with or without fursultiamine (20, 50, and 100 μM) for 12 hours and were subjected to immunoblotting for HIF-1α and β-actin. (**E**) Primary hRPE cells subjected to hypoxia with or without fursultiamine (50 μM) for 12 hours were fixed and stained with Tom20 antibody to visualize mitochondrial membranes (*arrows*). $^{*}P < 0.05$ versus LPS only; $^{\#}P < 0.05$ versus control ($n = 3$ per group). *Scale bar*: 10 μm.

Investigative Ophthalmology & Visual Science

Warburg effect. This metabolic switch also occurs in effector T helper lymphocytes[36] and activated macrophages.[37] When energy metabolism shifts from OXPHOS to glycolysis, the RPE is placed under metabolic stress, decreasing its ability to support the retina.[38] Furthermore, enhancing mitochondrial activity makes the RPE more resilient to oxidative damage, further supporting the important role of RPE mitochondria.[28] Palsson-McDermott et al.[12] reported that inhibiting LPS-induced metabolic reprogramming attenuates secretion of inflammatory cytokines. Thus, the anti-inflammatory effect of fursultiamine could be due to modulation of RPE metabolism, suggesting the potential of fursultiamine as a novel AMD therapeutic.

The active form of thiamine, thiamine diphosphate, is an essential cofactor of several enzymes important for mitochondrial energy metabolism, including PDH.[39] In the current study, fursultiamine increased maximal and spare OCR in LPS-treated ARPE-19 cells. Metabolic reprogramming that enhances glycolysis and impairs OXPHOS has been implicated in inflammatory processes, as the shift from OXPHOS to glycolysis increases pro-IL-1β expression and generation of reactive oxygen species.[40] This immunometabolic disease mechanism was supported by a recent study, which demonstrated that both genetic and pharmacological inhibition of mitochondrial PDH kinase isozymes improves mitochondrial function and decreases expression of proinflammatory cytokines.[41] Taken together, our data suggest that fursultiamine disrupted metabolic reprogramming from OXPHOS to aerobic glycolysis, which could be associated with the attenuated inflammatory response in the RPE.

Interestingly, fursultiamine enhancement of mitochondrial activity in LPS-treated cells peaked at 20 µM, whereas its suppressive effect on cytokine secretion peaked at 100 µM. This could be because the potentiated mitochondrial activity after pyruvate supplementation, indicated by increased basal OCR, sensitized ARPE-19 cells to the fursultiamine. Furthermore, the shift in mitochondrial energy metabolism could precede changes of cytokine protein levels. These data indicate that, by enhancing the mitochondrial activity, fursultiamine could prevent the shift from oxidative to glycolytic metabolism under inflammatory conditions.

Andre et al.[29] reported that tissue hypoxia is observed as early as day 3 after CNV induction in the CNV mouse model. Moreover, HIF-1α expression is upregulated in the RPE surrounding CNV lesions, together with increased VEGF expression.[42] These findings indicate that RPE hypoxia and tissue ischemia are involved in the progression of CNV. We also confirmed that in ARPE-19 cells hypoxia increased HIF-1α and VEGF expression in vitro. In hypoxic conditions where OXPHOS is impaired, HIF-1α promotes aerobic glycolysis by regulating transcription of lactate dehydrogenase and pyruvate dehydrogenase kinases, which phosphorylate and therefore inhibit PDH.[31] Interestingly, Minchenko et al.[43] reported that in human RPE cells hypoxia induces HIF-1α-dependent upregulation of glycolytic enzymes, including 6-phosphofructo-2-kinase/fructose-2,6-bisphosphatase-3, regulating the Warburg effect. Furthermore, in the mouse CNV model, targeted disruption of HIF-1α in the RPE attenuates VEGF upregulation, alleviating CNV.[42] Consistent with these findings, the present study identified that hypoxia increased phosphorylated PDH levels and lactate production in the RPE, which are indicative of metabolic reprogramming. This effect was reversed by fursultiamine. Further, fursultiamine treatment enhanced mitochondrial metabolism and decreased VEGF expression, which would alleviate CNV. These findings suggest that fursultiamine could suppress metabolic reprogramming by enhancing OXPHOS, which would be correlated with decreased NF-κB activation and HIF-1α stabilization. Taken together, these findings demonstrated that mitochondrial function in a complex microenvironment mediated by inflammation and/or hypoxia is a potential therapeutic target to alleviate pathological neovascularization in neovascular AMD.

We did not compare the therapeutic effects of fursultiamine with those of other B1 derivatives, as doing so was out of the scope of the present study. However, prior studies reported that lipophilic thiamine derivatives such as fursultiamine exhibit improved bioavailability compared to water-soluble derivatives such as thiamine nitrate.[44] Furthermore, fursultiamine has improved systemic exposure and faster absorption relative to benfotiamine.[45] A phase 2 clinical trial (NCT02423811) to evaluate the effect of fursultiamine in esophageal squamous cell carcinoma patients, completed in 2017,[46] should reduce safety concerns in future translational studies on fursultiamine. Thus, it is possible that the lipophilic nature of fursultiamine could be advantageous to the protective effect of thiamine, and researchers will progress to translational studies and clinical trials to evaluate the therapeutic value of fursultiamine in exudative AMD patients.

The etiology of neovascular AMD is complex, and both inflammation and hypoxia contribute to the pathological processes that culminate in neovascularization. In the present study, we demonstrated that fursultiamine decreased inflammatory cytokine levels both in vivo in CNV mice and in vitro in human RPE cells, and we found that these effects could be mediated by mitochondria metabolism. Furthermore, our data support a therapeutic role for fursultiamine in CNV that is related to suppression of inflammatory cytokine production arising from inflammatory and hypoxic pathological processes in neovascular AMD.

Acknowledgments

The authors thank Kip M. Connor, PhD, Angiogenesis Laboratory, Department of Ophthalmology, Massachusetts Eye & Ear, Harvard Medical School, for his guidance with the CNV model.

DHP is financially supported by the Basic Science Research Program of the National Research Foundation of Korea, funded by the Ministry of Science and ICT, Republic of Korea (2019R1A2C1084371), and by the Korea Health Technology R&D Project of the Korea Health Industry Development Institute, funded by the Ministry of Health & Welfare, Republic of Korea (HI16C1501).

Disclosure: **J.Y. Do**, None; **J. Kim**, None; **M.-J. Kim**, None; **J.Y. Lee**, None; **S.-Y. Park**, None; **R. Yanai**, None; **I.-K. Lee**, None; **S. Park**, None; **D.H. Park**, None

References

1. Gehrs KM, Anderson DH, Johnson LV, Hageman GS. Age-related macular degeneration–emerging pathogenetic and therapeutic concepts. *Ann Med*. 2006;38(7):450–471.
2. Ambati J, Fowler BJ. Mechanisms of age-related macular degeneration. *Neuron*. 2012;75(1):26–39.

3. Strauss O. The retinal pigment epithelium in visual function. *Physiol Rev*. 2005;85(3):845–881.
4. Jarrett SG, Lin H, Godley BF, Boulton ME. Mitochondrial DNA damage and its potential role in retinal degeneration. *Prog Retin Eye Res*. 2008;27(6):596–607.
5. Delori FC, Goger DG, Dorey CK. Age-related accumulation and spatial distribution of lipofuscin in RPE of normal subjects. *Invest Ophthalmol Vis Sci*. 2001;42(8):1855–1866.
6. Sparrow JR, Boulton M. RPE lipofuscin and its role in retinal pathobiology. *Exp Eye Res*. 2005;80(5):595–606.
7. Nordgaard CL, Karunadharma PP, Feng X, Olsen TW, Ferrington DA. Mitochondrial proteomics of the retinal pigment epithelium at progressive stages of age-related macular degeneration. *Invest Ophthalmol Vis Sci*. 2008;49(7):2848–2855.
8. Howes KA, Liu Y, Dunaief JL, et al. Receptor for advanced glycation end products and age-related macular degeneration. *Invest Ophthalmol Vis Sci*. 2004;45(10):3713–3720.
9. Wang XC, Jobin C, Allen JB, Roberts WL, Jaffe GJ. Suppression of NF-kappaB-dependent proinflammatory gene expression in human RPE cells by a proteasome inhibitor. *Invest Ophthalmol Vis Sci*. 1999;40(2):477–486.
10. Bian ZM, Elner VM, Yoshida A, Kunkel SL, Elner SG. Signaling pathways for glycated human serum albumin-induced IL-8 and MCP-1 secretion in human RPE cells. *Invest Ophthalmol Vis Sci*. 2001;42(7):1660–1668.
11. Izumi-Nagai K, Nagai N, Ozawa Y, et al. Interleukin-6 receptor-mediated activation of signal transducer and activator of transcription-3 (STAT3) promotes choroidal neovascularization. *Am J Pathol*. 2007;170(6):2149–2158.
12. Palsson-McDermott EM, Curtis AM, Goel G, et al. Pyruvate kinase M2 regulates Hif-1α activity and IL-1β induction and is a critical determinant of the Warburg effect in LPS-activated macrophages. *Cell Metab*. 2015;21(1):65–80.
13. Imtiyaz HZ, Simon MC. Hypoxia-inducible factors as essential regulators of inflammation. *Curr Top Microbiol Immunol*. 2010;345:105–120.
14. Zera K, Sweet R, Zastre J. Role of HIF-1α in the hypoxia inducible expression of the thiamine transporter, SLC19A3. *Gene*. 2016;595(2):212–220.
15. Lonsdale D. A review of the biochemistry, metabolism and clinical benefits of thiamin(e) and its derivatives. *Evid Based Complement Alternat Med*. 2006;3(1):49–59.
16. Yadav UC, Kalariya NM, Srivastava SK, Ramana KV. Protective role of benfotiamine, a fat-soluble vitamin B1 analogue, in lipopolysaccharide-induced cytotoxic signals in murine macrophages. *Free Radic Biol Med*. 2010;48(10):1423–1434.
17. Bozic I, Savic D, Laketa D, et al. Benfotiamine attenuates inflammatory response in LPS stimulated BV-2 microglia. *PLoS One*. 2015;10(2):e0118372.
18. Satish S, Philipose H, Rosales MAB, Saint-Geniez M. Pharmaceutical induction of PGC-1α promotes retinal pigment epithelial cell metabolism and protects against oxidative damage. *Oxid Med Cell Longev*. 2018;2018:9248640.
19. Hasegawa E, Inafuku S, Mulki L, et al. Cytochrome P450 monooxygenase lipid metabolites are significant second messengers in the resolution of choroidal neovascularization. *Proc Natl Acad Sci USA*. 2017;114(36):E7545–E7553.
20. Yanai R, Mulki L, Hasegawa E, et al. Cytochrome P450-generated metabolites derived from ω-3 fatty acids attenuate neovascularization. *Proc Natl Acad Sci USA*. 2014;111(26):9603–9608.
21. Oh H, Takagi H, Takagi C, et al. The potential angiogenic role of macrophages in the formation of choroidal neovascular membranes. *Invest Ophthalmol Vis Sci*. 1999;40(9):1891–1898.
22. Grossniklaus HE, Ling JX, Wallace TM, et al. Macrophage and retinal pigment epithelium expression of angiogenic cytokines in choroidal neovascularization. *Mol Vis*. 2002;8:119–126.
23. Bretz CA, Divoky V, Prchal J, et al. Erythropoietin signaling increases choroidal macrophages and cytokine expression, and exacerbates choroidal neovascularization. *Sci Rep*. 2018;8(1):2161.
24. Leung KW, Barnstable CJ, Tombran-Tink J. Bacterial endotoxin activates retinal pigment epithelial cells and induces their degeneration through IL-6 and IL-8 autocrine signaling. *Mol Immunol*. 2009;46(7):1374–1386.
25. Cui H-S, Li Y-M, Fang W, Li J-K, Dai Y-M, Zheng L-S. Effect of berberine on lipopolysaccharide-induced monocyte chemotactic protein-1 and interleukin-8 expression in a human retinal pigment epithelial cell line. *Int Ophthalmol*. 2018;38(5):2053–2060.
26. Adijanto J, Philp NJ. Cultured primary human fetal retinal pigment epithelium (hfRPE) as a model for evaluating RPE metabolism. *Exp Eye Res*. 2014;126:77–84.
27. Miceli MV, Newsome DA, Schriver GW. Glucose uptake, hexose monophosphate shunt activity, and oxygen consumption in cultured human retinal pigment epithelial cells. *Invest Ophthalmol Vis Sci*. 1990;31(2):277–283.
28. Iacovelli J, Rowe GC, Khadka A, et al. PGC-1α induces human RPE oxidative metabolism and antioxidant capacity. *Invest Ophthalmol Vis Sci*. 2016;57(3):1038–1051.
29. Andre H, Tunik S, Aronsson M, Kvanta A. Hypoxia-inducible factor-1α is associated with sprouting angiogenesis in the murine laser-induced choroidal neovascularization model. *Invest Ophthalmol Vis Sci*. 2015;56(11):6591–6604.
30. Zhang P, Wang Y, Hui Y, et al. Inhibition of VEGF expression by targeting HIF-1 alpha with small interference RNA in human RPE cells. *Ophthalmologica*. 2007;221(6):411–417.
31. Pearce EL, Pearce EJ. Metabolic pathways in immune cell activation and quiescence. *Immunity*. 2013;38(4):633–643.
32. Pacal L, Kuricova K, Kankova K. Evidence for altered thiamine metabolism in diabetes: is there a potential to oppose gluco- and lipotoxicity by rational supplementation? *World J Diabetes*. 2014;5(3):288–295.
33. Xie F, Cheng Z, Li S, et al. Pharmacokinetic study of benfotiamine and the bioavailability assessment compared to thiamine hydrochloride. *J Clin Pharmacol*. 2014;54(6):688–695.
34. Bitsch R, Wolf M, Möller J, Heuzeroth L, Grüneklee D. Bioavailability assessment of the lipophilic benfotiamine as compared to a water-soluble thiamin derivative. *Ann Nutr Metab*. 1991;35(5):292–296.
35. Elner VM, Strieter RM, Elner SG, Baggiolini M, Lindley I, Kunkel SL. Neutrophil chemotactic factor (IL-8) gene expression by cytokine-treated retinal pigment epithelial cells. *Am J Pathol*. 1990;136(4):745–750.
36. Chang CH, Curtis JD, Maggi LB, et al. Posttranscriptional control of T cell effector function by aerobic glycolysis. *Cell*. 2013;153(6):1239–1251.
37. Rodriguez-Prados JC, Traves PG, Cuenca J, et al. Substrate fate in activated macrophages: a comparison between innate, classic, and alternative activation. *J Immunol*. 2010;185(1):605–614.
38. Kurihara T, Westenskow PD, Gantner ML, et al. Hypoxia-induced metabolic stress in retinal pigment epithelial cells is sufficient to induce photoreceptor degeneration. *Elife*. 2016;5:e14319.
39. Gangolf M, Czerniecki J, Radermecker M, et al. Thiamine status in humans and content of phosphorylated thiamine derivatives in biopsies and cultured cells. *PLoS One*. 2010;5(10):e13616.
40. Van den Bossche J, O'Neill LA, Menon D. Macrophage immunometabolism: where are we (going)? *Trends Immunol*. 2017;38(6):395–406.

Investigative Ophthalmology & Visual Science

41. Min BK, Park S, Kang HJ, et al. Pyruvate dehydrogenase kinase is a metabolic checkpoint for polarization of macrophages to the M1 phenotype. *Front Immunol*. 2019;10:944.
42. Lin M, Hu Y, Chen Y, et al. Impacts of hypoxia-inducible factor-1 knockout in the retinal pigment epithelium on choroidal neovascularization. *Invest Ophthalmol Vis Sci*. 2012;53(10):6197–6206.
43. Minchenko A, Leshchinsky I, Opentanova I, et al. Hypoxia-inducible factor-1-mediated expression of the 6-phosphofructo-2-kinase/fructose-2,6-bisphosphatase-3 (PFKFB3) gene. Its possible role in the Warburg effect. *J Biol Chem*. 2002;277(8):6183–6187.
44. Kitamori N, Itokawa Y. Pharmacokinetics of thiamin after oral administration of thiamin tetrahydrofurfuryl disulfide to humans. *J Nutr Sci Vitaminol (Tokyo)*. 1993;39(5):465–472.
45. Park WS, Lee J, Hong T, et al. Comparative pharmacokinetic analysis of thiamine and its phosphorylated metabolites administered as multivitamin preparations. *Clin Ther*. 2016;38(10):2277–2285.
46. National Cheng-Kung University Hospital. Fursultiamine in esophageal squamous cell carcinoma patients who receive concurrent chemoradiotherapy. Available at: https://clinicaltrials.gov/ct2/show/NCT02423811. Accessed October 14, 2020.